Day-ahead offering strategy in the market for concentrating solar power considering thermoelectric decoupling by a compressed air energy storage

Shitong Sun[a], Seyed Mahdi Kazemi-Razi[b], Lisa G. Kaigutha[c], Mousa Marzband[c,d], Hamed Nafisi[b], Ameena Saad Al-Sumaiti[e]

[a]*China-EU Institute for Clean and Renewable Energy, Huazhong University of Science and Technology, Wuhan 430074, PR China*
[b]*Department of Electrical Engineering, Amirkabir University of Technology, Tehran, Iran*
[c]*Northumbria University, Electrical Power and Control Systems Research Group, Ellison Place NE1 8ST, Newcastle upon Tyne, United Kingdom*
[d]*Center of Research Excellence in Renewable Energy and Power Systems, King Abdulaziz University, Jeddah 21589 Saudi Arabia*
[e]*Advanced Power and Energy Center, Electrical Engineering and Computer Science, Khalifa University, P.O. Box: 127788, Abu Dhabi, United Arab Emirates*

Abstract

Due to limited fossil fuel resources, a growing increase in energy demand and the need to maintain positive environmental effects, concentrating solar power (CSP) plant as a promising technology has driven the world to find new sustainable and competitive methods for energy production. The scheduling capability of a CSP plant equipped with thermal energy storage (TES) surpasses a photovoltaic (PV) unit uncertainties and augments the sustainability of energy system performance. However, restricting CSP plant application compared to a PV plant due to its high investment is a challenging issue. This paper presents a model to assemble a combined heat and power (CHP) with a CSP plant for enhancing heat utilization and reduce the overall cost of the plant, thus, the CSP benefits proved by researches can be implemented more economically. Moreover, the compressed air energy storage (CAES) is used with a CSP-TES-CHP plant in order that the thermoelectric decoupling of the CHP be facilitated. Therefore, the virtual power plant (VPP) created is a suitable design for large power grids, which can trade heat and electricity in re-

Email address: mousa.marzband@northumbria.ac.uk Corresponding author (Mousa Marzband)

sponse to the market without restraint by thermoelectric constraint. Furthermore, the day-ahead offering strategy of the VPP is modeled as a mixed integer linear programming (MILP) problem with the goal of maximizing the profit in the market. The simulation results prove the efficiency of the proposed model. The proposed VPP has a 2% increase in profit and a maximum 6% increase in the market electricity price per day compared to the system without CAES.

Keywords: Combined heat and power, compressed air energy storage, concentrating solar power, thermal energy storage, virtual power plant.

Nomenclature

A. Acronyms

BT	back-pressure turbine
CAES	compressed air energy storage
CHP	combined heat and power
CSP	concentrating solar power
DER	distributed energy resource
ISO	independent system operator
KKT	Karush-Kuhn-Tucker
PCM	phase change material
PV	photovoltaic
TES	thermal storage system
VPP	virtual power plant

B.Indices

t	time-step index
s	scenario index
i	electricity generator index
j	heat generator index
d	electricity load index
k	heat load index

C. Constant variables

η^{BT}	the efficiency of the BT $[-]$
η^{TES+} / η^{TES-}	the heat charging/ discharging efficiency of the TES $[-]$

η^{CSP}	the heat transfer efficiency of the CSP [−]
η^{CAES+}/ η^{CAES-}	storing/ generation efficiency of CAES [−]
γ	the dissipation coefficient [−]
k	thermoelectric ratio of the BT [−]
Δt	time interval [h]
$\overline{P}^{BT}$/ $\underline{P}^{BT}$	max/ min electrical power of BT [kW]
$\overline{P}^{TES+}$/ $\overline{P}^{TES-}$	max generation/ storing capacity of TES [kWh]
$\overline{E}^{TES}$/ $\underline{E}^{TES}$	max/ min energy capacity of the TES [kWh]
$\underline{T}^{BTON}$/ $\underline{T}^{BTOFF}$	min ON/ OFF times of the BT [h]
$\overline{RU}^{BT}$/ $\overline{RD}^{BT}$	max upward/downward ramping rate of electrical power from the BT [kW]
$\underline{P}^{CAES+}$/ $\underline{P}^{CAES-}$	min storage/ generation capacity of CAES [kW]
$\overline{P}^{CAES+}$/ $\overline{P}^{CAES-}$	max storage/ generation capacity of CAES [kW]
$\overline{E}^{CAES}$/ $\underline{E}^{CAES}$	max/ min energy capacity of the CAES [kWh]
$E^{CAES}_{s(ini)}$	initial energy stored of the CAES [kWh]
P^{load}_{st}	power consumption [kW]
Q^{load}_{st}	heat consumption [kW]
M^{P}	constant variable defining the dispatched power limits [kW]
$M^{\mu P}$	constant variable defining the electricity price limits [£/kWh]
M^{Q}	constant variable defining the dispatched heat limits [kW]
$M^{\mu Q}$	constant variable defining the heat price limits [£/kWh]

D. Decision variables

P^{BT}_{st}/Q^{BT}_{st}	the power/ heat output of the BT [kW]
$P^{TES+}_{st}/P^{TES-}_{st}$	the TES heat charging/discharging power [kW]
u^{CSP}_{st}	the on/off state of the CSP-CHP [-]
P^{BTSU}	the heat loss power of the BT starts up [kW]
P^{solar}_{st}	the solar field power [kW]
E^{TES}_{st}	the stored energy of the TES [kWh]
$u^{TES+}_{st}/u^{TES-}_{st}$	the charging/discharging state of the TES [$\in$(0,1)]
u^{BT}_{st}	startup state variable of the BT [$\in$(0,1)]
x^{BT}_{st}	the on/off state variable of the BT [$\in$(0,1)]

$u_{st}^{CAES+}/u_{st}^{CAES-}$	binary storage/generation status indicator of CAES [$\in(0,1)$]
$P_{st}^{CAES+}/P_{st}^{CAES-}$	storing/generation power of CAES [kW]
E_{st}^{CAES}	power stored in CAES unit [kWh]
$P_{st}^{BT,net}/P_{st}^{BT,load}/$ $P_{st}^{BT,CAES}$	power from BT to energy market/ load/ CAES [kW]
$P_{st}^{CAES,net}/P_{st}^{CAES,load}$	power from CAES to energy market/ load [kW]
$P_{st}^{net,CAES}/P_{st}^{net,load}$	power from energy market to CAES/ load [kW]
$Q_{st}^{net,load}$	heat from energy market to load [kW]
$Q_{st}^{BT,net}/\ Q_{st}^{BT,load}$	heat from BT to energy market/ load [kW]
P_{ist}^{G}	power generation of the unit *i* accepted by the ISO [kW]
P_{dst}^{D}	load of the load *d* accepted by the ISO [kW]
Q_{jst}^{G}	thermal generation of the unit *j* accepted by the ISO [kW]
Q_{kst}^{D}	thermal of the load k accepted by the ISO [kW]
$\lambda_{st}^{e}/\lambda_{st}^{th}$	electricity/thermal price in MCP [$/kWh]
$\pi_{ist}^{PG}/\pi_{dst}^{PD}$	electricity offer price of the unit *i*/ load *d* [£/kWh]
$\pi_{jst}^{QG}/\pi_{kst}^{QD}$	thermal offer price of the unit *j*/ load *k* [£/kWh]
$\overline{P}_{ist}^{G}/\overline{P}_{dst}^{D}$	offer quantity of the unit *i*/ load *d* [kW]
$\overline{Q}_{jst}^{G}/\overline{Q}_{kst}^{D}$	thermal offer quantity of the unit *j*/ load *k* [kW]
$\overline{\mu}_{ist}^{PG}/\ \underline{\mu}_{ist}^{PG}$	max/ min value of electricity offer price of the unit *i* [kW]
$\overline{\mu}_{dst}^{PD}/\ \underline{\mu}_{dst}^{PD}$	max/ min value of electricity bid price of the load *d* [kW]
$\overline{\mu}_{jst}^{QG}/\ \underline{\mu}_{jst}^{QG}$	max/ min value of heat offer price of the unit *j* [kW]
$\overline{\mu}_{kst}^{QD}/\ \underline{\mu}_{kst}^{QD}$	max/ min value of heat bid price of the load *k* [kW]
$\overline{\omega}_{ist}^{PG}/\ \underline{\omega}_{ist}^{PG}$	auxiliary variable for offer electricity price and quantity upper/lower level [-]
$\overline{\omega}_{dst}^{PD}/\ \underline{\omega}_{dst}^{PD}$	auxiliary variable for bid electricity price and quantity upper/lower level [-]
$\overline{\omega}_{jst}^{QG}/\ \underline{\omega}_{jst}^{QG}$	auxiliary variable for offer heat price and quantity upper/lower level [-]
$\overline{\omega}_{kst}^{QD}/\ \underline{\omega}_{kst}^{QD}$	auxiliary variable for bid heat price and quantity upper/lower level [-]
ϕ^{ON}/ϕ^{OFF}	end of period in BT ON/OFF status constraints [h]

1. Introduction

1.1. Motivation

A significant percentage of electricity is generated by burning fossil fuels [1]. Due to the limited amount and high cost of fossil fuels, the need to reduce greenhouse gases emissions from fossil fuels burning and climate change, the intensified energy crisis, the increased energy consumption as a result of industrialization, urbanization and economic development in developing countries such as China in recent years, as well as rising electricity prices, investing in renewable energy is an option to ensure a secure and sustainable energy supply. Therefore, the attention of scientists around the world has been attracted to improving energy conversion techniques and increasing the efficiency and flexibility (using hybrid storage) of renewable production [2]. The advantages of renewable energy include easy accessibility, widespread abundance, environmental friendliness, low prices and clearness even in rural areas [3]. Renewable energies include solar thermal energy (e.g. concentrating solar power (CSP) technology), photovoltaic (PV), wind turbine, bioenergy, as well as hydro power. Solar energy can be easily converted into heat and electricity and can be stored as heat. Given the stated advantages, reduction in cost of installation and production of solar power in recent years, as well as in accordance with the Paris agreement and the existing subsidies allocated [4], its investment has increased rapidly [5] (growth rate of about 2.6% per year from 2012 (as 200 GW installed until 2019) and 28.89% renewable energy (3.55% PV power and 0.07% CSP power) out of a total of 6399 GW global consumption at the end of 2019 [6]). The CSP, as an energy conversion technology, collects solar energy using a set of reflectors mounted toward a receiver to provide superheated steam (with an intermediate fluid such as molten salt) and drive the turbo generator [7]. The CSP power generation process, with an efficiency of about 40.5% [8], also generates exhaust steam with a low or medium temperature range. In addition, CSP stores fuel and thus eliminates environmental pollutant emissions. CSP is more efficient and less expensive than fuel consuming units such as diesel generator [9]. Also, compared to PV, their output power is smoother due to higher inertia and a 87%

reduction in CO_2 emissions allows CSP to participate in the CO_2 emissions market and have minor impact on the environment. Unlike PV, CSP technology does not have the overheating problem and the complexity of its solutions, and therefore their use increases especially in hot areas. Since solar power has an inherent periodicity, it can be combined with other strategies to form a hybrid system, deal with the periodic nature and provide reliable energy, especially in island mode. These strategies include different energy storages such as batteries, compressed air energy storage (CAES), pump storage, thermal-compressed supercritical carbon dioxide storage, thermal storage, fuel cell vehicle, as well as phase change material (PCM) [10, 11]. Due to the conversion of solar energy into thermal energy in CSP technology, storing energy as heat is the most common method in the application of this technology [1]. By integrating with CSP, thermal storage system (TES) enables it to produce full power capacity even in some hours without solar power, which provides flexible scheduling characteristics for CSP plant [12].TES improves thermal comfort, reduces battery storage especially in island mode and makes smoother the heat load profiles by providing the ability of flexible supplement of electrical and thermal loads [13]. By adding combined heat and power (CHP) to CSP-TES, the strategy of generating electricity and heat simultaneously via the waste heat in exhaust steam, improves the energy resource utilization and thus make CSP investment profitable, given high initial investment cost of CSP [14, 15]. As a result, improving the use of CSP as a energy resource help to implement the CSP-TES-CHP energy system and exploit the CSP advantages proved in the previous relevant researches. Heat supply in addition to electricity using CSP-TES-CHP reduces the need for equipment such as gas boiler and thus decreases fuel consumption and air pollution. Moreover, by providing heat load (including temperature and hot water), the need for power-to-heat converter equipment that reduces process efficiency is eliminated [16]. Because high-efficiency CHP technology allows for the reduction of primary energy consumption and CO_2 emissions, the 2004/8/EC directive [17] has supported the use of CHP in European countries. Due to the intermittency and probability of CSP output, the system needs more flexibility to penetrate CSP energy. Systematic integration of hybrid power and heating systems to achieve their coordi-

nated planning and performance concurrently, increases flexibility [18] and allows more CSP energy to penetrate [1]. CSP equipped with TES, alongside the CHP, forms a single complex called the virtual power plant (VPP). A VPP is like a power plant connected to the transmission system that consists of several distributed energy resources (DERs) and creates a single operational profile by combining the parameters of these DERs. VPP profile (similar to traditional power plants) is defined by a set of characteristics including scheduled generated power, constraints such as power rates, cost characteristics, as well as reserve. In addition to DERs, VPP can coordinate controllable loads using tools such as demand elasticity and electrical load recovery strategies to form a more flexible profile. Using this profile, the individual power plant can communicate directly with any market participant to make purchase/sale contracts, offer services (e.g. power power balancing and ancillary services including frequency and voltage regulation) and decentralize the system management. The separate performance of each DER does not provide sufficient capacity and flexible controls to make an optimal system management and minimum cost in market participation, as well as feasible performance with respect to technical constraints [19], while these problems have been fixed by VPP. Because of the CSP output power with heterogeneous spatial distribution and daily intermittency and increased cost in the event of unforeseen changes in power [20], the optimal planning and performance scheduling of the integrated system is important to improve robustness and high-efficiency performance . For optimal performance scheduling in a VPP, an internal VPP energy management strategy that addresses the appropriate offering in the market [21] and also improves the cost of the VPP is essential. However, the thermoelectric constraint resulting from the high correlation between the electrical power and the heating steam volume of the CHP limits the electrical and thermal power of the VPP and reduces its profit in market participation [22]. As a result, how to improve system flexibility through thermoelectric decoupling is a necessity. CAES is based on the use of cheap electricity (during off-peak hours such as night or during high electricity generation hours) to compress air and store it in large tanks, then release compressed air at times of higher electricity demand to turn the turbine for electricity generation. The efficiency of the CAES

storage process is up to about 54% (which is lower compared to pump storage) and has a long life (more than 20 years) [23]. Due to the need for huge amounts of air and as a result of economic constraints, only natural reservoirs (e.g. salt caves and limestone mines) are currently economical [23]. With electricity storage, CAES can improve grid performance, balance power consumption curve, as well as achieve thermoelectric decoupling capability in multi-energy systems [24].

1.2. Literature review

There is a valuable literature in the field of using CSP technology and its participation in the competitive market, each of which has tried to reduce the effect of its power uncertainty, using exhaust steam, decouple thermoelectric constraint of electrical/thermal power generated or provide optimal offers in the market. The paper presented in [25] improves the performance of systems including solar sources in the presence of the probabilities of these sources and shows that the probabilities are effective in the performance and cost of the system. Due to the error in predicting solar radiation as a result of air pollution, Ref. [26] presents an modified ASHRAE model. In this model, the values of air temperature, humidity rate, air quality and relative humidity are specified as improving parameters. The results demonstrate that this model compared to the traditional ASHRAE model, improves the Nash sutcliffe equation by 27.17% and reduces the root mean square error by 55.99%. The results of the investigation in [27] prove that storing the surplus electricity can provide 100% renewable generation (including solar), increase energy security, reduce the power curtailment and increase the flexibility. Also, pump storage and fuel cell [28] joint with solar plants, has been proven for suppressing the solar plants variability. Furthermore, the integration of PV plants with wind turbine reduces the effects of solar power intermittence [29]. The addition of thermal power plants to the solar-wind complex has also improved this trend [30]. Similarly, Huang *et al.* [31] have proven that integrating hydropower with PV-wind improves their power uncertainties. Jurasz *et al.* [32] have demonstrated the use of hydropower in improving PV uncertainties, and the integrated set as a price taker in the market, makes more profit during market participation. But Refs. [31, 32]

do not consider the heating network and technologies of CSP, CHP, as well as CAES. The effect of integration of batteries, electric vehicles bidirectional charging station and commercial buildings with PV units has been investigated to decrease the impact of PV power probabilities and system costs in the framework presented in [33]. Moreover, the real-time control ability in this framework increases resilience to unpredictable conditions and electric vehicles owners participation. However, in the study conducted in Ref. [33], the high-efficiency technologies of CSP, CHP as well as the heating network are not considered. Yan et al. [1] examine the feasibility of using a TES for an island-based PV-wind turbine-electrical storage system in Hong Kong and suggests a new PCM with a $Ba(OH)_2.8H_2O$ structure used to manage the system thermal power. But, CSP and CHP technologies as well as offering strategies in the market are not included in this model. The scheduling model proposed in Ref. [18] minimizes the cost of a PV-wind turbine-CHP system in which, due to the PV and wind turbine probabilities, the probabilistic spinning reserve is presented in the form of a chance-constrained. The proposed model reduces the curtailment of PV and wind turbine resources, which are the result of the traditional heat-set modes of CHP, by improving the operation flexibility. Thermal comfort and buildings inertia are also included in thermal load modeling. Cocco et al. [34] prove that the combination of PV and TES with CSP plants can guarantee the provision of a constant value for the output power of the hybrid system over a longer period despite the uncertainties in solar power. In addition, the efficiency and capacity of CSP is increased. This strategy also eliminates the need for expensive battery banks by storing the thermal energy type to store solar power fluctuation. The techno-economic impact of TES and natural gas integrated into CSP for reducing the CSP output power probabilities effect is also investigated in [35]. The CSP-TES-electric heater systems coordinated with a wind farm in [36, 37], cope with the variability and study self-scheduling for maximizing the profit of the electricity/ancillary services market participation (in addition, a 100% reduction in wind curtailment is resulted in [36]). Refs. [14, 15] use a CHP (BT) unit integrated with CSP-TES to increase system efficiency by waste heat utilization. The presented combined heat and power scheduling provides both electrical and thermal loads simultane-

ously. Also, an energy storage buildings equipped with PCMs is used in [14] to facilitate thermoelectric decoupling. The heating and cooling storage quantity of PCMs enhances the conventional thermal power plants operational economy and heat generation units. This mode of operation is used in isolated CSP-CHP plants (commonly used in remote areas) and leads to lower cost and improved potential, however, it has not paid attention to market participation and large scale systems. Due to the importance of PCMs, Ref. [11] increases the heat absorption efficiency of PCM by constructing heat transfer networks mimicking leaf veins. Thus, the heat absorption efficiency is increased to 196.67% compared to metal foam enhanced PCM plate. In addition to providing thermal load, the waste heat in exhaust steam generated in CSP technology can also feed desalination units in a combined CSP-wind turbine-desalination system [9] to produce fresh water and improve the use of energy resources. As a result, in addition to improving overall energy utilization, part of the electricity demand for desalination is effectively transferred to the thermal load and the electricity demand is reduced. However, this method does not use high-efficiency CHP technology for using the exhaust steam. VPP is researched in [19] to determine its ability to improve the performance of aggregated DERs in both system management and market participation. This paper presents decentralized energy management frameworks and market participation of DERs using the aggregation of DERs in a VPP to demonstrate the impact of its key features on the optimal management of DERs. Also, risk management and qualifying the capabilities of aggregated DERs for optimizing their operating costs are shown. The model presented in [38] provides day-ahead scheduling and optimal bidding strategies for a CSP participating in the day-ahead market. Furthermore, the probabilities of price market and CSP power are taken account. A molten salt thermal storage is used for providing electricity production even during hours without solar radiation to increase CSP penetration. However, it has not used CHP for using the waste heat, thus, the maximum overall energy utilization is not achieved. In addition to modeling CSP-TES offering strategy in the energy market, its participation in the ancillary services market (including the reserve and regulation market) is also considered in [39]. In Ref. [40], the authors present a bi-level model for energy management

of DERs, in which at the lower level the DERs optimal decentralized dispatch are specified and at the upper level, the electricity surplus/shortage of each section is sent to a central unit. But these references do not pay attention to CSP technology. The model presented in Ref. [41] provides the ability of optimal day-ahead scheduling for multi-energy DERs of VPP and optimal offering for purchasing/selling in the energy market, however, CSP technology is not paid attention. The authors in [42] have shown that the storage flexibility used in an integrated set participating in a competitive market allows for better offering. But in this paper, the heating network is not considered. In addition to not paying attention to the market clearing price process, the technologies of CSP, CHP and CAES, as well as the VPP concept have not been studied. The hybrid energy storage system, including thermochemical technology (using Cobalt monoxide) and CAES in Ref. [43], increases round-trip efficiency and total exergy efficiency to 56.4% and 75.6%, respectively. Despite the many advantages of CAES in storage applications, only two high power CAESs are currently exploited: 1) McIntosh (with the capacity of 110 MW) installed in Alabama, USA, as well as 2) Huntorf (with the capacity of 321 MW) installed in Germany [24].

1.3. Contributions

Nonetheless, there is still a drawback to a systematic model for large scale CSP-CHP plant scheduling that also participates in the electricity and heat markets. Table 1 provides an at-a-glance view of the previous papers and shows their defects. Given the above, there are several gaps in the existing literature, which are listed as follows:

1. Considering previous work where a CSP is assembled with a CHP, the CSP-CHP plant electricity/heat output are coupled, and as a result the minimum available cost is not achieved. This is because the price of both the electricity and heat markets are effective on CSP-CHP plant power management and its electrical and thermal power cannot be scheduled independently based on the relevant market price.

Table 1: A comparative summary of this study and previous papers

Ref.	Equipment		Energy storage		VPP	Load	Thermoelectric	optimal	Market clearing price
	CSP	CHP	TES	CAES	concept	supply	decoupling	offering	
[26]	✖	✖	✖	✖	✖	electrical/thermal	✖	✖	✖
[27]	✖	✖	✖	✖	✖	electrical/thermal	✖	✖	✖
[1]	✖	✖	✖	✓	✖	electrical/thermal	✖	✖	✖
[18]	✖	✓	✓	✖	✖	electrical/thermal	✖	✖	✖
[35]	✓	✖	✓	✖	✖	electrical/thermal	✖	✖	✖
[36]	✓	✖	✓	✖	✖	electrical/thermal	✖	✖	✖
[14]	✓	✓	✓	✖	✖	electrical/thermal	✓	✖	✖
[37]	✓	✖	✓	✖	✖	electrical/thermal	✖	As a price-taker	✖
[9]	✓	✖	✓	✖	✖	electrical/thermal	✖	✖	✖
[19]	✖	✖	✖	✖	✓	electrical	✖	as a price-taker	✖
[39]	✓	✖	✓	✖	✖	electrical/thermal	✖	as a price-taker	✖
[41]	✖	✖	✖	✖	✓	electrical	✖	as a price-taker	✖
[43]	✓	✖	✓	✓	✖	electrical/thermal	✖	✖	✖
[31]	✖	✖	✖	✖	✖	electrical	✖	✖	✖
[32]	✖	✖	✖	✖	✖	electrical	✖	as a price-taker	✖
[42]	✖	✖	✖	✖	✖	electrical	✖	✓	✖
This study	✓	✓	✓	✓	✓	electrical/thermal	using CAES	as a price-maker	using KKT

2. There is no comprehensive price offering strategy to maximize CSP-CHP plant profits alongside market clearing.

This paper proposes a bi-level optimization model in order to optimally offer strategies for a CSP-CHP plant in large scale participation in the market. Therefore, the major contributions of this paper are:

1. The use of a CAES with a CSP-TES-CHP plant to decouple the electricity and heat generated by it as much as possible and eliminating thermoelectric constraint. This achieved innovative system leads to optimal use of energy resources.
2. Creating a single VPP including CSP-TES-CHP plant and CAES, and providing an optimization model for optimal day-ahead VPP portfolio offering strategies in the market. The presented model allows the VPP for being a price-maker, which aims to maximize its own profit. In addition, the market clearing process performed by the independent system operator (ISO) is considered along with the process of maximizing the VPP profit performed by the VPP operator.

2. Proposed idea

2.1. CSP-CHP plant

Figure 1 illustrates the CSP-CHP plant schematic. The CSP-CHP plant is made of a CSP, TES, thermal cycling system and back pressure combined heat and power turbine (BT). The molten salt is mainly used to transfer energy in the CSP plant. The heat transfer fluid guarantees energy transfer in the above subsystems. The heat transfer medium absorbs the energy from the solar field and its temperature rises to 520°C-560°C. During the molten salt transfer process, the CSP-CHP plant operator stores some of the heat in the TES and transfer the rest of heat to the thermal cycling unit (Eq. (1)). This second part of heat is for producing superheated steam through a 3 stage heat exchange in order to increase the efficiency of heat transfer from molten salt to water for producing steam. After the heat exchange, the molten salt temperature drops to 280°C-320°C and the molten salt returns to the solar field. The steam at a temperature of 535°C is transferred to the BT for generating electricity at the determined BT efficiency (Eq. (1)). Concurrently, the high-temperature exhaust steam generated by BT can be used for supplying the heat demand of industrial part or providing heating for residential part (in the steam-water heat exchanger). Therefore, by optimal use of energy resources, industrial and domestic use of energy is supplied economically. Even the superfluous thermal energy is used by the absorption refrigeration systems for the cooling supply, if there is no thermal load in summer. The steam also returns to the thermal cycling system after losing heat in the BT and passing through the condenser to reach the preset temperature, and the cycle continues.

2.2. A VPP based on CSP-CHP plant and CAES

There is a highly correlation between the CSP-CHP plant power generation and the heating steam volume, which can be solved effectively by implementing CAES alongside the CSP-CHP plant. CAES is an emerging "Bulk Energy Storage" technology where typically generated energy is stored during off-peak periods and dispatched to the electric grid during peak demand periods. CAES is used to separate

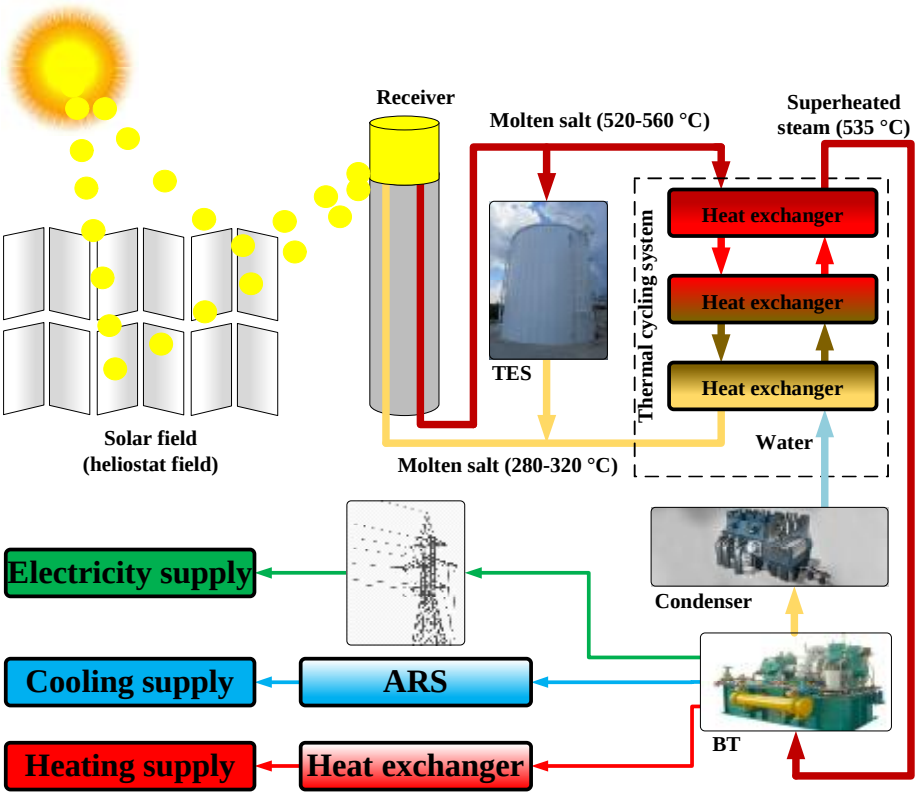

Figure 1: Energy transfer process in the CSP-CHP plant.

electricity and heat produced by CSP-CHP and reducing the interaction between the electricity-thermal market, while maximising electric and heat profit of the VPP. Therefore, CAES is operable in two modes, a) Charging, in which air undergoes compression through the use of power from the CSP-CHP or the electricity market, b) Discharging, in which the air that has been stored in the earlier mode (charging) is utilized for powering the gas turbine and selling it to the electricity market. At the same time, CAES can purchase electricity from the electricity market when the electricity price is relatively low and sell it when electricity price is relatively high. CAES is a receiver of power for air compression in underground salt cavities. It utilizes the compressed air as an air expander for generating electricity. Although CAES, like TES, can improve power supply during hours without solar radiation, it should be noted that the purpose of using CAES is to decouple the thermoelectric constraint of electricity and heat output of CSP-TES-CHP (which are interdependent with a thermoelectric ratio). As a result, electricity and heat at the VPP output can be changed independently, and the VPP operator determines their value based on the price of electricity and heat. While the molten salt TES used in the CSP-TES-CHP, is not able to decouple the thermoelectric constraint. The CSP-CHP plant and CAES complex can be considered as a single VPP. Based on the European project FENIX [44], the quantity of DERs capacity can be aggregated by VPP. Then, an operating power profile from combining the parameters corresponding to each DER is created and VPP can consider the network effect on aggregated DER power. The VPP internal power and thermal flow is shown in Figure 2. Determining the optimal bidding strategy in the market (in the form of a proposal with a dual parameter of price and amount of energy) is necessary for the VPP operator to maximize VPP profit through participating in the markets. A bi-level optimization model is proposed for the day-ahead offering strategy of the VPP, which aims at profit maximization (Eqs. (33)- (40)). Furthermore, the VPP operator must pay attention to the VPP constraints that result from the combination of constraints of the CSP-CHP plant and CAES (Eqs. (23)-(32)). Figure 2 shows that part of the CSP-CHP plant power ($P_t^{BT,net}$) is sold directly to the market by the VPP operator and part of ($P_t^{BT,CAES}$) is stored in the VPP's internal CAES (Eq. (27)).

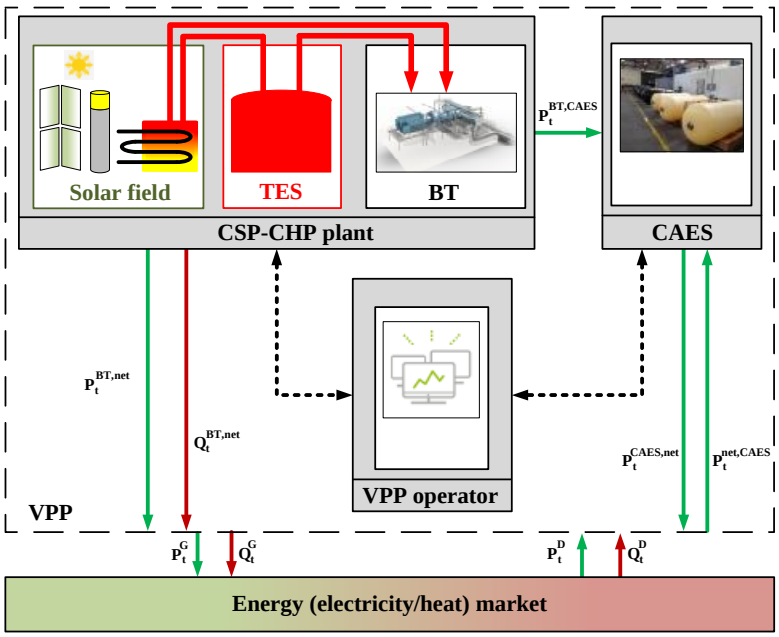

Figure 2: Schematic view of the VPP.

The VPP operator is also able to sell part of the CAES energy ($P_t^{CAES,net}$) to the market or buy power ($P_t^{net,CAES}$) from the market to store in the CAES. In addition, the heat generated in BT (Q_t^G) can be sold in the heat market. In order to determine the VPP participation in the electricity and heat market in the next 24 hours, the VPP proposal for each time-step of the next day must be notified to the ISO, as shown Figure 3, so that the ISO can be based on it and also the offers of other VPPs and loads, while specifying the scheduled purchase/sell power of VPP (P_t^G, Q_t^G, P_t^D, Q_t^D) for the next day. Section 4 illustrates the lower cost of the presented VPP.

2.3. Optimization process

In order to consider both the profit of a VPP and the clearing of the electricity market, a bi-level optimization model has been elaborated in order to optimally offer strategies for the VPP , as shown in Figure 3. Here, it is assumed that in all power plants participating in the market, the proposed model from the point of view of VPP *i* (the VPP under study) deals via optimal bidding in the market to maximize its

profit. The input data of the proposed model is the value of the parameters related to the CSP, TES, BT unit, CAES and other plants and loads (Tables (2)-(3)). The upper level takes the VPP's profit maximization as the optimization goal (Eq. (33)), while considering the VPP operation constraints (Eqs. (23)-(32)). In addition, the bidding strategy of the VPP participating in the electricity and heat market is determined (including the price and amount of energy offered to ISO), then passed to the lower level. The lower level receives the VPP *i* bidding for each time-step of the next day. Moreover, it receives bidding of other power plants and loads. The lower level is used as the constraint of the upper level, and the market focuses on maximizing social welfare, as an objective function (Eq. (34)). Furthermore, the constraints existing in the market clearing (Eqs. (35)-(40)) must be met. The lower level has an impact on the operating schedule of the upper level by returning the clearing price of the market to the upper level. The day before market clearing price is the dual variable of the node power balance equation in the lower layer problem. After sending the price and energy dispatched for each time-step to upper level, the VPP operator plans the power of VPP to maximize its profits. Finally, the proposed model output includes the net power purchased/sold of VPP *i*, as well as the net power of CSP-CHP plant and CAES in each time-step.

3. Methods

3.1. Mathematical model of the CSP-CHP plant

3.1.1. The CSP-CHP plant power balance

The CSP-CHP plant power balance is described in Eq. (1). The power received from the sun at the CSP plant receiver, which is shown in Figure 1 (P_t^{solar}) is equivalent to the power received in BT (P_t^{BT}/η^{BT}), the power dissipated in BT (P^{BTSU}), as well as the net power received by TES.

$$P_{st}^{BT}/\eta^{BT} - P_{st}^{TES-}\eta^{TES-} + P_{st}^{TES+}/\eta^{TES+} + u_{st}^{CSP}P^{BTSU} = P_{st}^{solar}\eta^{CSP} \tag{1}$$

Eq. (2) determines the BT heating capacity, which is come from the exhaust steam, therefore Eq. (1) does not include Q_t^{BT}. It is related to the unit active power

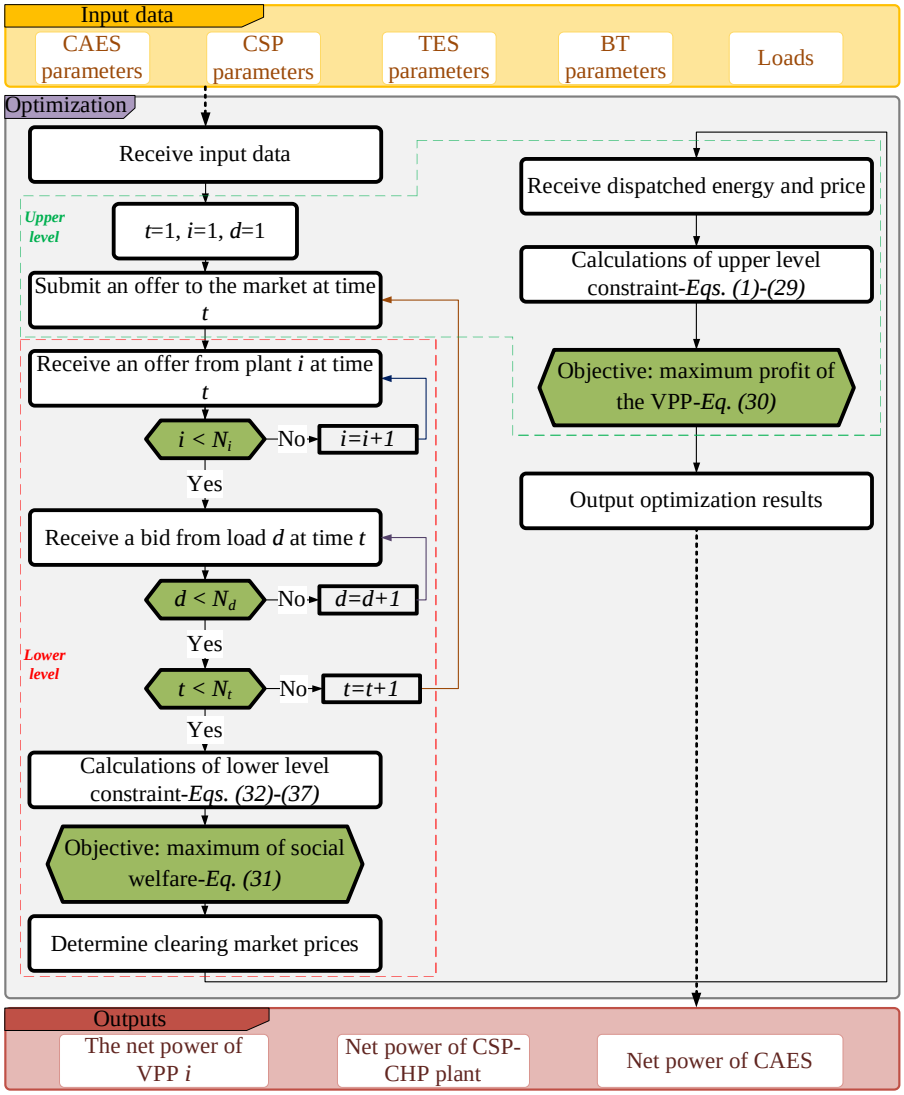

Figure 3: Bi-level optimization model framework.

(P_t^{BT}) by a constant coefficient. Eqs. (1) and (2) model the energy conversion process in CSP-TES-CHP unit.

$$Q_{st}^{BT} = kP_{st}^{BT} \tag{2}$$

3.1.2. The equations of TES of the CSP plant

At time *t*, The TES energy capacity is depended on the power of charging and discharging and also its capacity (E_{t-1}^{TES}) at time *t*-1 (Eq. 3), while Eq. (4) shows that the minimum/maximum capacity of the TES constrains its capacity ($\underline{E}^{TES}$/ $\overline{E}^{TES}$).

$$E_{st}^{TES} = (1-\gamma)E_{s(t\text{-}1)}^{TES} + (P_{s(t-1)}^{TES+} - P_{s(t-1)}^{TES\text{-}})\Delta t \tag{3}$$

$$\underline{E}^{TES} \leqslant E_{st}^{TES} \leqslant \overline{E}^{TES} \tag{4}$$

The charging/discharging power of TES is constrained by its maximum power at each moment (Eqs. (5)-(6)). It is notable that the process of charging and discharging can not be done simultaneously, which is considered by (7). When TES is charging/ discharging, the u_t^{TES+}/ $u_t^{TES\text{-}}$ is 1 respectively and the other one is 0.

$$0 \leqslant P_{st}^{TES+} \leqslant u_{st}^{TES+}\overline{P}^{TES+} \tag{5}$$

$$0 \leqslant P_{st}^{TES\text{-}} \leqslant u_{st}^{TES\text{-}}\overline{P}^{TES\text{-}} \tag{6}$$

$$u_{st}^{TES+} + u_{st}^{TES\text{-}} \leqslant 1 \tag{7}$$

3.1.3. BT constraints

Eqs. (8)-(11) define the constraints of start and stop time of BT, respectively. The constraints of power ramping of the CSP-CHP unit are also implemented by Eqs. (12)-(15). In Eq. (16), the output power of BT is limited via ($\underline{P}^{BT}$/ $\overline{P}^{BT}$), which specifies the standard range of BT power. Given Eq. (2), it is concluded that Eq. (16) also shows a range on the Q_t^{BT}.

$$x_{st}^{BT} - x_{s(t\text{-}1)}^{BT} \leqslant x_{s\tau}^{BT}, \forall\tau \in \left\{t+1, \phi^{ON}\right\} \tag{8}$$

$$\phi^{ON} = \begin{cases} t + \underline{T}^{BTON} - 1, (t + \underline{T}^{BTON} - 1) < T \\ T, (t + \underline{T}^{BTON} - 1) > T \end{cases} \tag{9}$$

$$x_{s(t\text{-}1)}^{BT} - x_{st}^{BT} \leqslant 1 - x_{s\tau}^{BT}, \forall\tau \in \left\{t+1, \phi^{OFF}\right\} \tag{10}$$

$$\phi^{OFF} = \begin{cases} t + \underline{T}^{BTOFF} - 1, (t + \underline{T}^{BTOFF} - 1) < T \\ T, (t + \underline{T}^{BTOFF} - 1) > T \end{cases} \tag{11}$$

$$x^{BT}_{st} - x^{BT}_{s(t-1)} \leqslant u^{BT}_{st} \tag{12}$$

$$u^{BT}_{st} \leqslant x^{BT}_{st} \tag{13}$$

$$u^{BT}_{st} \leqslant 1 - x^{BT}_{s(t-1)} \tag{14}$$

$$-\overline{RD}^{BT} \leqslant P^{BT}_{st} - P^{BT}_{s(t-1)} \leqslant \overline{RU}^{BT} \tag{15}$$

$$\underline{P}^{BT} \leqslant P^{BT}_{st} \leqslant \overline{P}^{BT} \tag{16}$$

3.2. Modelling of the CAES

Eq. (17) necessitates that is not to be in operation in both the charging and discharging modes at the same time. While Eqs. (18)- (19) restrict the CAES power consumption and generation to their corresponding up limit, respectively ($\overline{P}^{CAES-}$, $\overline{P}^{CAES+}$). u^{CAES-}_{t}/ u^{CAES+}_{t} are equal to 1 at the charge/ discharge time of CAES and 0 at other times, respectively. The initial amount of energy stored in CAES is determined according to Eq. (20). The hourly CAES energy balance is represented by Eq. (21). CAES energy at each time-step depends on the charging power, discharging power and its energy at the previous time step. Finally, Eq. (22) states the CAES energy storage limits. It is evident that Eqs. (17)- (22) show the 1^{st} contribution in Section 1.3 [45, 46].

$$u^{CAES+}_{st} + u^{CAES-}_{st} \leqslant 1 \tag{17}$$

$$u^{CAES+}_{st}\underline{P}^{CAES+} \leqslant P^{CAES+}_{st} \leqslant u^{CAES+}_{st}\overline{P}^{CAES+} \tag{18}$$

$$u^{CAES-}_{st}\underline{P}^{CAES-} \leqslant P^{CAES-}_{st} \leqslant u^{CAES-}_{st}\overline{P}^{CAES-} \tag{19}$$

$$E^{CAES}_{s(t=1)} = E^{CAES}_{s(ini)} \tag{20}$$

$$E^{CAES}_{st} = E^{CAES}_{s(t-1)} + P^{CAES+}_{st}\eta^{CAES+} - \frac{P^{CAES-}_{st}}{\eta^{CAES-}} \tag{21}$$

$$\underline{E}^{CAES} \leqslant E^{CAES}_{st} \leqslant \overline{E}^{CAES} \tag{22}$$

3.3. The VPP portfolio

Eqs. (23)-(32) represent the hourly power balance of the VPP. Theses equations represent the 2nd contribution in Section 1, and combine the equations of CSP-CHP plant (Eqs. (1)- (16)) and CAES (Eqs. (17)- (22)) to form the VPP. According to Eq. (23), the production power of the VPP is equal to the production power of CSP-CHP plant and CAES. Eq. (24) indicates that the power purchased from the market by the VPP operator is used to supply the loads or stored in CAES. Due to the lack of heat storage outside the CSP-CHP plant, the heat generated by the VPP is equal to the heat generated by BT (Eq. 25), and the heat purchased is only to supply the thermal load (Eq. 26). The VPP operator adjusts the BT power to equal the total load power, the power to be stored in the CAES, and the power sold to the market by BT (Eq. 27).

$$P_{st}^{G} = P_{st}^{BT,net} + P_{st}^{CAES,net} \tag{23}$$

$$P_{st}^{D} = P_{st}^{net,load} + P_{st}^{net,CAES} \tag{24}$$

$$Q_{st}^{G} = Q_{st}^{BT,net} \tag{25}$$

$$Q_{st}^{D} = Q_{st}^{net,load} \tag{26}$$

$$P_{st}^{BT} = P_{st}^{BT,load} + P_{st}^{BT,CAES} + P_{st}^{BT,net} \tag{27}$$

$$Q_{st}^{BT} = Q_{st}^{BT,net} + Q_{st}^{BT,load} \tag{28}$$

The charging/ discharging power of CAES when located in a VPP is in accordance with the Eqs. (29)- (30), respectively. The electrical load is supplied by CAES, the market purchase and BT (Eq. 31), while Eq. (32) shows that the thermal load can only be supplied by the heat market and BT.

$$P_{st}^{CAES+} = P_{st}^{BT,CAES} + P_{st}^{net,CAES} \tag{29}$$

$$P_{st}^{CAES-} = P_{st}^{CAES,load} + P_{st}^{CAES,net} \tag{30}$$

$$P_{st}^{load} = P_{st}^{CAES,load} + P_{st}^{net,load} + P_{st}^{BT,load} \tag{31}$$

$$Q_{st}^{load} = Q_{st}^{net,load} + Q_{st}^{BT,load} \tag{32}$$

3.4. Two levels of optimization problem

3.4.1. Objective function

As stated in Section 1 and Section 2.3, for solving this optimization problem, a bi-level model is proposed . The proposed model includes an upper and lower level for representing the maximization of VPP profit (Eq. (33) as objective function) and the market clearing process of ISO (Eq. (34) as objective function), respectively. Eq. (33) leads to economic industrial/domestic use of energy in the VPP as well as determines the optimal power of resources located in the VPP and the amount of power exchanges with the electricity/heat market. The replacement of the lower level by its first order Karush-Kuhn-Tucker (KKT) conditions are allowed, because a linear problem is used to model the lower level. This formulation uses the strong duality theory and KKT conditions [47] to present a mathematical program with equilibrium conditions that is converted into a mixed integer linear programming (MILP) model. The upper level objective function is in the form of revenue minus the cost of the VPP from participating in the electricity and heat markets. λ_t^e and λ_t^{th} are prices in the electricity and heat markets, respectively. The lower level objective function is social welfare and includes the electrical and thermal power of all power plants and loads. All eight components of Eq. (34) are the lower level output, which are the price and energy quantity dispatched for all power plants and loads, and is eventually sent to the corresponding power plant or load in the upper level.

$$\max \left\{ \sum_{t\in T, I\in I^S, D\in D^S} \lambda_{st}^e (P_{ist}^G - P_{dst}^D) + \sum_{t\in T, j\in J^S, k\in K^S} \lambda_{st}^{th} (Q_{jst}^G - Q_{kst}^D) \right\} \quad (33)$$

$$\min \left\{ \sum_{i\in I, t\in T} \pi_{ist}^{PG} P_{ist}^G - \sum_{d\in D, t\in T} \pi_{dst}^{PD} P_{dst}^D + \sum_{j\in J, t\in T} \pi_{jst}^{QG} Q_{jst}^G - \sum_{k\in K, t\in T} \pi_{kst}^{QD} Q_{kst}^D \right\} \quad (34)$$

3.4.2. Constraints

The dual variables of Eqs. (35)- (40) are defined according to their allowable limits and the objective function in the Eq. (34). Eqs. (35) and (36) represent the power balance constraint for the entire system. Moreover, Eqs. (37)- (38) respectively reflect the electricity generation and consumption offer quantity constraints

of the VPP as well as its rivals, while Eqs. (39)- (40) defines these constraints for heat generation and consumption offer quantity.

$$\sum_{d\in D,t\in T} P^{D}_{dst} = \sum_{i\in I,t\in T} P^{G}_{ist} : \lambda^{e}_{st} \tag{35}$$

$$\sum_{k\in K,t\in T} Q^{D}_{kst} = \sum_{j\in J,t\in T} Q^{G}_{jst} : \lambda^{th}_{st} \tag{36}$$

$$0 \leqslant P^{G}_{ist} \leqslant \overline{P}^{G}_{ist} : \underline{\mu}^{PG}_{ist}, \overline{\mu}^{PG}_{ist} \tag{37}$$

$$0 \leqslant P^{D}_{dst} \leqslant \overline{P}^{D}_{dst} : \underline{\mu}^{PD}_{dst}, \overline{\mu}^{PD}_{dst} \tag{38}$$

$$0 \leqslant Q^{G}_{jst} \leqslant \overline{Q}^{G}_{jst} : \underline{\mu}^{QG}_{jst}, \overline{\mu}^{QG}_{jst} \tag{39}$$

$$0 \leqslant Q^{D}_{kst} \leqslant \overline{Q}^{D}_{kst} : \underline{\mu}^{QD}_{kst}, \overline{\mu}^{QD}_{kst} \tag{40}$$

3.4.3. KKT conditions of lower-level

The lower-level problem is recognized for its continuity and linearity. Therefore, its replacement by the corresponding KKT conditions is possible. The use of such equilibrium conditions back in the upper-level is recognized as a mathematical program with equilibrium constraints (MPEC), whose formulation is in the form of Eqs. (41)- (52).

$$\pi^{PG}_{ist} - \lambda^{e}_{st} - \underline{\mu}^{PG}_{ist} + \overline{\mu}^{PG}_{ist} = 0 \tag{41}$$

$$-\pi^{PD}_{dst} + \lambda^{e}_{st} - \underline{\mu}^{PD}_{dst} + \overline{\mu}^{PD}_{dst} = 0 \tag{42}$$

$$\pi^{QG}_{jst} - \lambda^{th}_{st} - \underline{\mu}^{QG}_{jst} + \overline{\mu}^{QG}_{jst} = 0 \tag{43}$$

$$-\pi^{QD}_{kst} + \lambda^{th}_{st} - \underline{\mu}^{QD}_{kst} + \overline{\mu}^{QD}_{kst} = 0 \tag{44}$$

$$0 \leqslant P^{G}_{ist} \perp \underline{\mu}^{PG}_{ist} \geqslant 0 \tag{45}$$

$$0 \leqslant \overline{P}^{G}_{ist} - P^{G}_{ist} \perp \overline{\mu}^{PG}_{ist} \geqslant 0 \tag{46}$$

$$0 \leqslant P^{D}_{ist} \perp \underline{\mu}^{PD}_{ist} \geqslant 0 \tag{47}$$

$$0 \leqslant \overline{P}^{D}_{ist} - P^{D}_{ist} \perp \overline{\mu}^{PD}_{ist} \geqslant 0 \tag{48}$$

$$0 \leqslant Q^{G}_{jst} \perp \underline{\mu}^{QG}_{jst} \geqslant 0 \tag{49}$$

$$0 \leqslant \overline{Q}^{G}_{jst} - Q^{G}_{jst} \perp \overline{\mu}^{QG}_{jst} \geqslant 0 \tag{50}$$

$$0 \leqslant Q^{D}_{kst} \perp \underline{\mu}^{QD}_{kst} \geqslant 0 \tag{51}$$

$$0 \leqslant \overline{Q}^{D}_{kst} - Q^{D}_{kst} \perp \overline{\mu}^{QD}_{kst} \geqslant 0 \tag{52}$$

3.4.4. Equivalent linear formulation using KKT model

Equivalent subject to linearization of the upper and lower level and considering profit maximization of VPP constraints can be expressed as Eq. (53), as an objective function. Eqs. (54)- (69) also determine the constraints of the equivalent optimization problem.

$$\begin{aligned}
&\max \left\{ \sum_{t\in T, I\in I^S, D\in D^S} \lambda^e_{st}(P^G_{ist} - P^D_{dst}) \right. \\
&+ \sum_{t\in T, j\in J^S, k\in K^S} \lambda^{th}_{st}(Q^G_{jst} - Q^D_{kst}) = \\
&\max \left\{ - \sum_{t\in T, i\in I^R} (\pi^{PG}_{ist} P^G_{ist} - \overline{\mu}^{PG}_{ist} \overline{P}^G_{ist}) \right. \\
&+ \sum_{t\in T, d\in D^R} (\pi^{PD}_{dst} P^D_{dst} - \overline{\mu}^{PD}_{dst} \overline{P}^D_{dst}) \\
&- \sum_{t\in T, j\in J^R} (\pi^{QG}_{jst} Q^G_{jst} - \overline{\mu}^{QG}_{jst} \overline{Q}^G_{jst}) \\
&+ \sum_{t\in T, k\in K^R} (\pi^{QD}_{kst} Q^D_{kst} - \overline{\mu}^{QD}_{kst} \overline{P}^D_{kst})
\end{aligned} \tag{53}$$

$$P^G_{ist} \leqslant (1 - \underline{\omega}^{PG}_{ist}) M^P \tag{54}$$

$$\underline{\mu}^{PG}_{ist} \leqslant \underline{\omega}^{PG}_{ist} M^{\mu P} \tag{55}$$

$$\overline{P}^G_{ist} - P^G_{ist} \leqslant (1 - \overline{\omega}^{PG}_{ist}) M^P \tag{56}$$

$$\overline{\mu}^{PG}_{ist} \leqslant \overline{\omega}^{PG}_{ist} M^{\mu P} \tag{57}$$

$$P^D_{dst} \leqslant (1 - \underline{\omega}^{PD}_{dst}) M^P \tag{58}$$

$$\underline{\mu}^{PD}_{dst} \leqslant \underline{\omega}^{PD}_{dst} M^{\mu P} \tag{59}$$

$$\overline{P}^D_{dst} - P^D_{dst} \leqslant (1 - \overline{\omega}^{PD}_{dst}) M^P \tag{60}$$

$$\overline{\mu}^{PD}_{dst} \leqslant \overline{\omega}^{PD}_{dst} M^{\mu P} \tag{61}$$

$$Q^G_{jst} \leqslant (1 - \underline{\omega}^{QG}_{jst}) M^Q \tag{62}$$

$$\underline{\mu}^{QG}_{jst} \leqslant \underline{\omega}^{QG}_{jst} M^{\mu Q} \tag{63}$$

$$\overline{Q}^G_{jst} - Q^G_{jst} \leqslant (1 - \overline{\omega}^{QG}_{jst}) M^Q \tag{64}$$

$$\overline{\mu}_{jst}^{QG} \leqslant \overline{\omega}_{jst}^{QG} M^{\mu Q} \tag{65}$$

$$Q_{kst}^{D} \leqslant (1 - \underline{\omega}_{kst}^{QD}) M^{Q} \tag{66}$$

$$\underline{\mu}_{kst}^{QD} \leqslant \underline{\omega}_{kst}^{QD} M^{\mu Q} \tag{67}$$

$$\overline{Q}_{kst}^{D} - Q_{kst}^{D} \leqslant (1 - \overline{\omega}_{kst}^{QD}) M^{Q} \tag{68}$$

$$\overline{\mu}_{kst}^{QD} \leqslant \overline{\omega}_{kst}^{QD} M^{\mu Q} \tag{69}$$

4. Results and discussion

4.1. The system used for assessing the proposed model

As stated in Section 1 and Section 2.3, a bi-level optimization model for the VPP day-ahead offering strategy in the electricity and heat market is presented in this paper, which maximizes its own profit (As shown in Figure 3).

For verifying the efficacy of the proposed optimal offering strategy of the VPP, the VPP in this paper is composed of a CSP-CHP plant and a CAES (Section 2.2). The technical data of the used VPP is shown in Tables 2 and 3. Table 2 shows the CSP plant specifications at the beginning of the VPP structure. Also, Table 2 sets out the TES parameters in CSP plant. The parameters of the BT for using exhausted steam are also shown in Table 2. Finally, Table 3 sets out the CAES parameters used, which include the characteristics of charging/discharging efficiency, rated power, allowed range of stored energy and initial stored energy, which are extracted from [48–50].

The power system used in this study includes twelve different rival generations and twelve load consumptions. Concurrently, the heat system includes another five different rival generations and six thermal load consumptions. These generators and loads along with the electricity and heat markets are shown in Figure 4. Figure 4 shows the VPP *i* whose profit is maximized at the upper level of the proposed model, is associated with both the electricity and heat markets, and its internal structure is as shown in Figure 2. To consider the uncertainty of probabilistic parameters including solar radiation and electrical and thermal loads, the backward scenario reduction algorithm is applied to the values of previous years of solar radiation (extracted form [51]) and electrical and thermal loads [14]. The result of

Table 2: Parameters of the CSP-TES-CHP unit

Equipment	Parameter	Value
CSP	heat transfer efficiency [%]	90
TES	heat charging efficiency [%]	98
	heat discharging efficiency [%]	98
	dissipation coefficient [%]	0.6
	ramping rate [MW/h]	300
	rated charging/discharging power [MW]	400
	minimum stored energy [MWh]	100
	maximum stored energy [MWh]	1500
	Initial stored energy [MWh]	800
BT	minimum downtime [h]	1
	minimum runtime [h]	1
	minimum output power [MW]	8
	maximum output power [MW]	80
	power efficiency [%]	37
	thermoelectric ratio [-]	1.07

Table 3: Parameters of the CAES

Parameter	Value
Charging efficiency [%]	98
Discharging efficiency [%]	98
Minimum charging/discharging power [MW]	0
Maximum charging/discharging power [MW]	120
Lower limit of stored energy [MWh]	200
Upper limit of stored energy [MWh]	1800
Initial stored energy [MWh]	1000

this algorithm is four scenarios for spring (S1), summer (S2), autumn (s3), as well as winter (S4), which are shown in Figures 5 and 6. The backward scenario reduction algorithm [52] also maintains the effect of the deleted scenarios, and as a result, the proposed model considers the risk of probabilistic parameters for each of the possible network conditions during the year and obtains the optimal result for each of these conditions. Moreover, reducing the number of scenarios with this algorithm increases the computing speed and also reduces the required computing volume. As mentioned, the amount of CSP output power in each scenario is as illustrated in Figure 5. Also, the installed CSP capacity is 100 MW. The electrical and thermal loads in each of the scenarios are shown in Figure 6 (the thermal load is the same in the spring and autumn scenarios). The electrical and thermal load for each of the other market participants shown in Figure 4, is assumed to be similar to Figure 6. It is assumed that each participant in the competitive market can offer a price between 0 to 200 $/MWh. Moreover, the low/up limit of power offering for generators and loads participating in the market (as shown in Figure 4) is 0 and 150 MW, respectively. In addition to generating power, the considered VPP that the upper level is implemented from its stand point, also has power consumption.

A MILP solver (CPLEX) is used in this paper for solving the VPP day-ahead scheduling. The scheduling cycle is 1 day, and each time-step is selected 1 hour.

4.2. Assessment modes definition

In order to present the superiority of the VPP composed of CSP-CHP and CAES, two modes of energy supply are considered, as shown in Table 4. In mode 1, the CSP-CHP plant and CAES as a single VPP is participated in the electricity market, moreover, the heat production of CSP-CHP plant is participated in the heat market. Besides, in mode 2 there is only the CSP-CHP plant, which participates in the electricity and heat market at the same time. Therefore, thermoelectric decoupling of CSP-CHP plant output power is not performed. In mode 1 compared to mode 2, the VPP operator optimizes the power and profit of the entire CSP-CHP plant and CAES suite, while in mode 2, only the CSP-CHP plant power scheduling is performed.

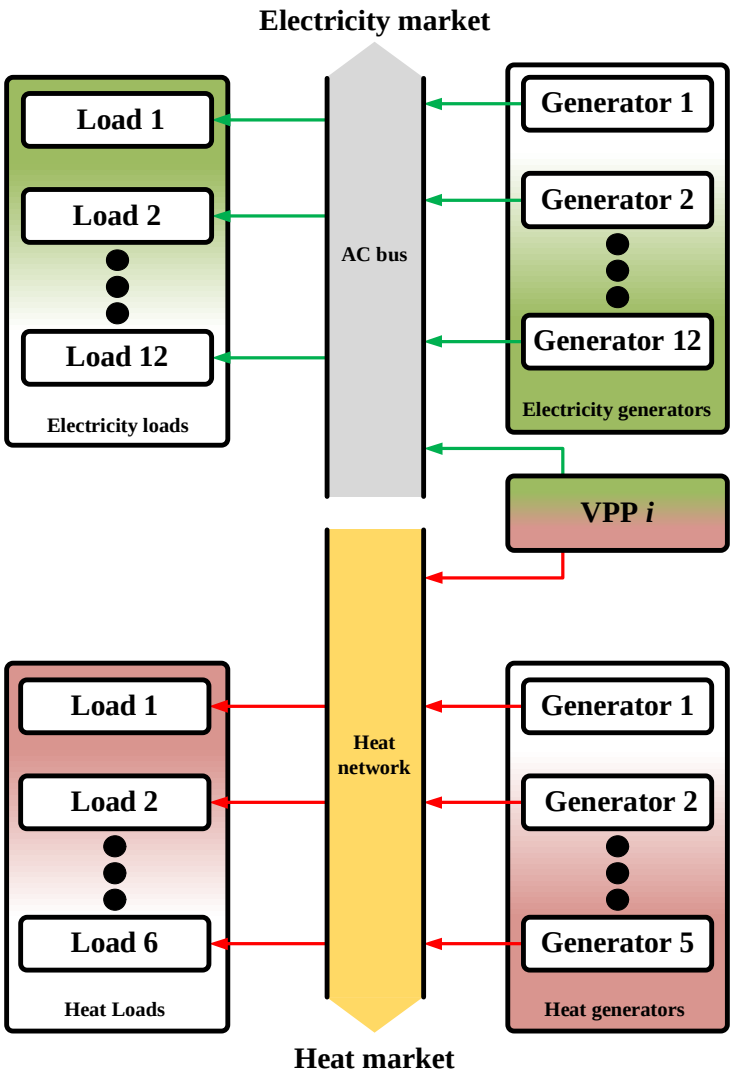

Figure 4: Electricity and gas prices on a winter day.

Table 4: Used modes definition

Mode	CSP-CHP plant	CAES	VPP concept
1	✓	✓	✓
2	✓	No	No

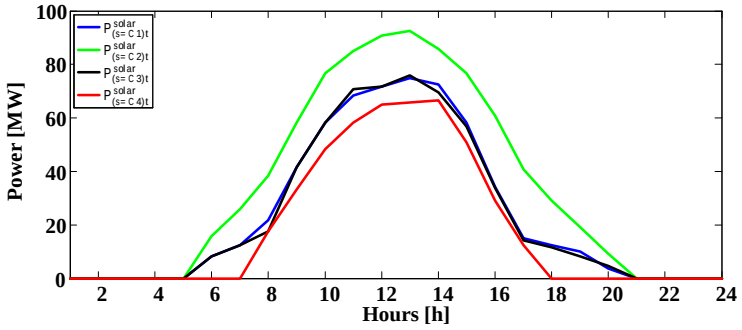

Figure 5: The output power of the CSP.

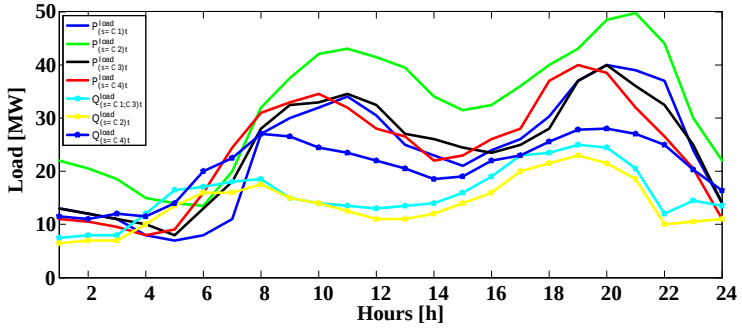

Figure 6: The electrical and thermal loads used for each market participant.

4.3. Comparison of power management and cleared prices in different modes

4.3.1. Power scheduling

Figure 7 shows the results of the VPP optimal strategy in next 24 hours for a typical winter day. It is noted that the power generation of the VPP has a great correlation with the system marginal electricity price, which is shown by the black curve in Figure 10. At high electricity prices (e.g. 06:00-10:00 and 17:00-22:00), the VPP tends to sell more electricity and maximize its own profit, while at lower electricity prices (e.g. 00:00-05:00, 15:00-17:00, and 23:00-24:00), the VPP tends to generate less electricity or even buy electricity from the electricity market. The stored electrical energy in CAES is used to resell to the market during peak electricity prices. As a result, the price difference between electricity purchased and sold to the market increases the VPP operator profit. It should be noted that in this power exchange, the VPP load (marked in yellow in Figure 7) must be fully supplied. Therefore, the power scheduling of the VPP in the upper level of the proposed model (Section 2.3), after determining the power and its price for the VPP in the lower level, leads to the powers of figure 7 for the internal components of the VPP. It is the responsibility of the VPP operator to communicate these amounts of powers to the relevant component and control their implementation in the VPP.

In terms of heat generation, the CAES part in the VPP can decouple electricity and heat of the CSP-CHP plant as much as possible. For example, Figure 7 shows at 16:00, the electrical power generation of the VPP is zero, but the heat generation is still high, indicating that electrical power generation of CSP-CHP plant is received by CAES.

The resulting CSP-CHP plant optimal strategy in mode 2 in the next 24 hours is illustrated in Figure 9. In mode 2, power generation does not exactly change with the electricity price (Figure 10), as in mode 1 (Figure 7). In addition, the relationship between heat and electricity generation in Figure 9 has always been the thermoelectricity ratio of BT, due to the lack of CAES in mode 2. The reason being that the electricity and heat of the CSP-CHP plant is strongly coupled, and the optimal scheduling of CSP-CHP plant must consider both electricity and heat

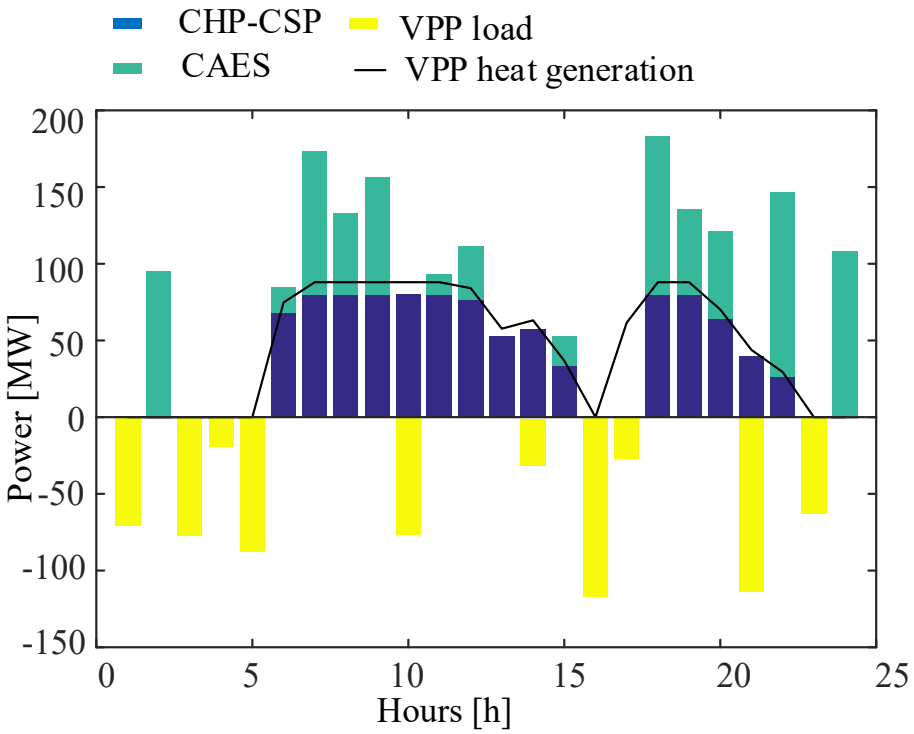

Figure 7: The optimal operation schedule in mode 1.

prices. Moreover, it is not possible to schedule the electrical power in a completely coordinated manner with the price of electricity. As a result, the freedom to schedule the power of the component in this mode is less and, therefore, its profit is less compared to the VPP (which uses CAES for thermoelectric decoupling), as shown in Table 5. The powers of Figure 9, like Figure 7, are determined in the upper level after the power and price of the CSP-CHP plant are determined in lower level (Section 2.3). Figure 8 shows the TES energy changes. During the period of 06:00-10:00, when the electricity price is high and as a result, the CSP-TES-CHP generation is high, the energy stores in CAES is reduced. But during hours such as 15:00-17:00 when the electricity price and CSP-TES-CHP generation is low and the production of solar field increases at the same time, the energy level of TES increases. TES stores the energy when the loads amount is low and the solar radiation is high to supply loads during the hours without solar radiation. Thus, it augments the

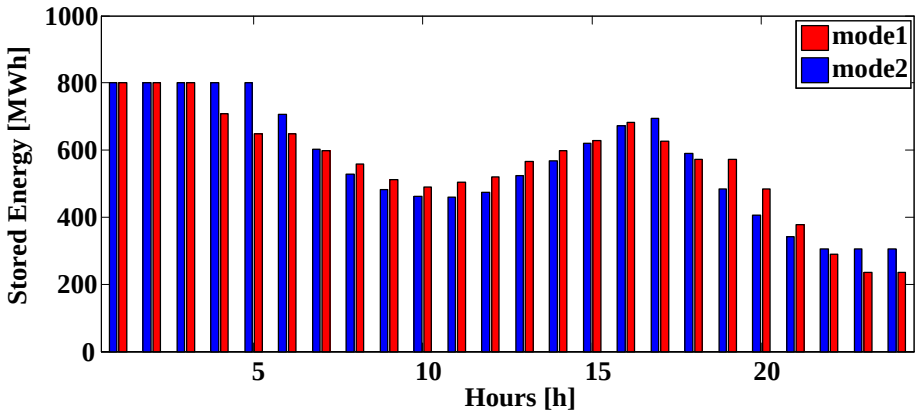

Figure 8: The stored energy of TES.

sustainability of energy system. As shown in Figure 8, in Mode 2, the TES energy level is lower in the middle of the day, because of generating more power by CSP-TES-CHP (its power changes are not optimal and are also affected by the price of heat) and lacking CAES to provide some of power consumption.

Due to the similarity of the results in each of the different scenarios (although the numbers vary in different scenarios of the year, but the results obtained by comparing them are similar) and also to avoid the complexity of the figures, only the winter scenario results are shown. Because in winter, there is the least solar radiation (Figure 5) and the highest thermal load (Figure 6) and it is the most critical scenario. Other weather-related conditions, such as cloudy weather with less solar radiation, can also be considered. The proposed model, due to the fact that the CSP-TES-CHP unit is connected to the electricity and heat market, can balance the power even for this case. But due to the lower CSP power generation, more power will be purchased from the market and the ability of CSP-TES-CHP to offer power in the market will be less. As a result, the profit of CSP-TES-CHP will be less compared to Table 5.

4.3.2. Cleared prices in electricity/heat market

Since electricity and heat can be decoupled in mode 1, the electricity price of the VPP is higher than mode 2, as shown in Figure 10. Consequently, the VPP is making

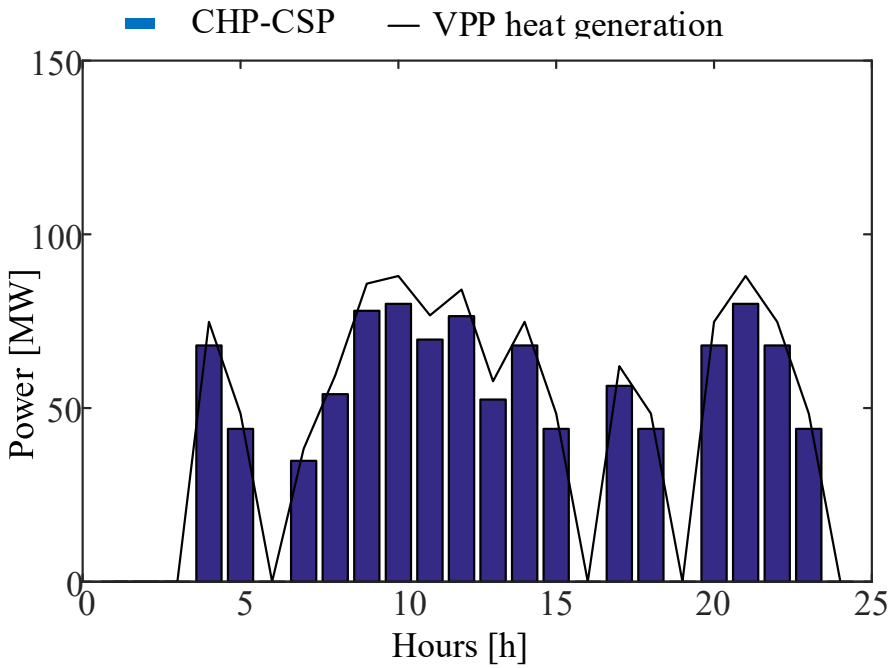

Figure 9: The optimal operation schedule in mode 2.

more profit than mode 2, which has not used CAES (Table 5). In both modes, the heat price remains the same but the electricity price is different indicating that in mode 1, the charge and discharge of CAES is used to control the electricity generated by the VPP to obtain a higher electricity price.

In mode 2, the price of electricity is lower than mode 1 (Figure 10), due to the limitation in power scheduling as a result of coupled electricity and heat generation, which is mentioned in part A of Section 4.3.

4.3.3. Comparison of profit

As shown in Table 5, the profit gain in mode 1 is higher than mode 2, indicating that mode 1 proposed in this paper has better economies of scale and schedulability. Since better scheduling capability makes the power of component inside the VPP according to the market electricity price, and with an aim of maximizing the VPP profit. But in mode 2, in addition to the electricity price, the heat price has also impacts on the component power. It is a constraint, which provides a lower profit

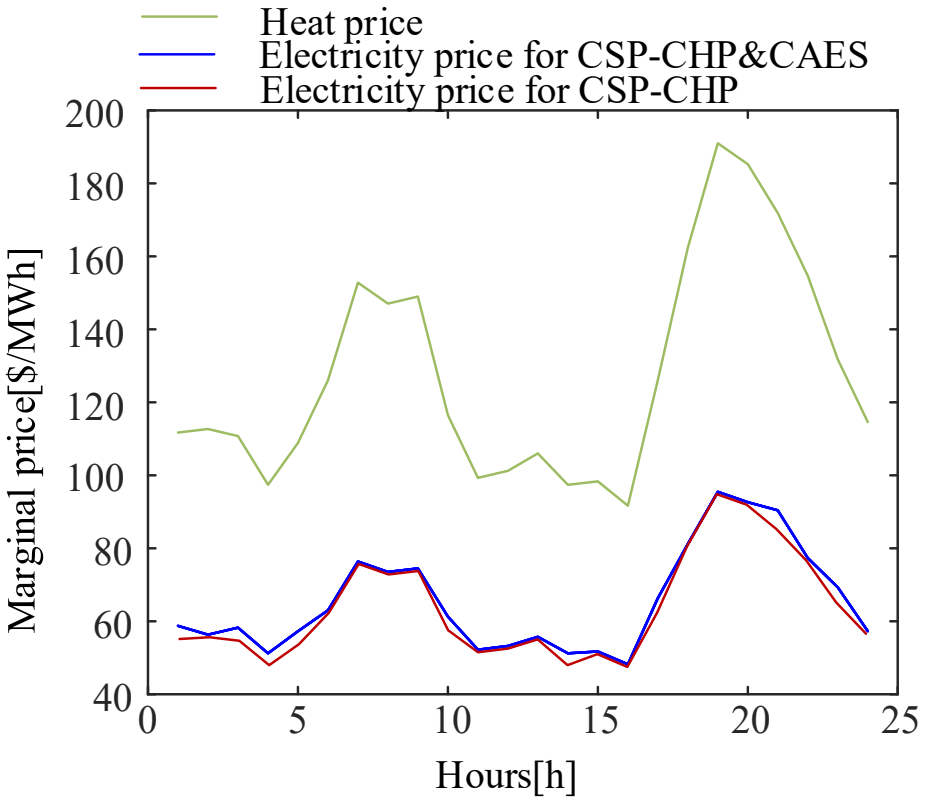

Figure 10: Electricity and heat market clearing price.

maximization than mode 1 (part A in Section 4.3). Therefore, according to Figure 7 and Table 5, CAES used in VPP makes an innovative system which creates this ability for the proposed model to use the energy sources more economically, while their technical constraints are also considered. As a result, the proposed model shows that implementation of VPP based on CAES has economical advantages, while it has also environmental advantages which are achieved using CSP and CHP, as it is explained in Section 1.1.

5. Conclusions

For improving the efficiency and reducing the overall cost of solar energy, this paper proposes a bi-level optimization model for optimal offering strategies of a

Table 5: Comparison of profit in two modes

Mode	Profit (k$)
1	1433.3
2	1405.8

VPP portfolio including a CSP-CHP plant and a CAES to supply electricity and also heat from the exhausted steam of the CHP unit. In addition, CAES is used for facilitating the thermoelectric decoupling of the CHP unit. It has been concluded that a detailed description of the CSP-CHP plant operation is presented and the mathematical model of the CSP-CHP plant alongside the CAES as a VPP, which participates in the market, is formulated via its KKT conditions.

To ensure the practical application of the proposed model, two modes, including VPP and another mode that does not use CAES are used on a network containing a number of generators and loads that participate in the electricity and heat market, and their results have been compared. The presented optimal offering strategies have promoted CSP-CHP plant participation in electricity markets in large power grids. The results show that the CAES part in the VPP can decouple electricity and heat of the CSP-CHP plant as much as possible, and the proposed VPP achieves higher profit. Also, the proposed VPP mitigates the environmental pollutants using CSP and CHP. The pivotal results of the proposed model are listed as follows:

1. The use of CAES has led to the decoupling of electricity and heat. As a result, in some hours, although the heat output is still high, the electrical power is zero and there is complete thermoelectric decoupling.
2. Electricity prices have risen by 5 $/MWh due to the use of CAES and thermoelectric decoupling.
3. The profit has been increased by 27,000 $ as a result of using CAES, compared to the mode without CAES.
4. An optimal model has been proposed for offering prices and power scheduling of a VPP, which also includes the price clearing mechanism in the electricity and heat market.

The suggested future work to be considered is how to use low-grade energy for seawater desalination or drinking water purification. Furthermore, how to come up with efficient and cost-effective ways to gain control of uncontrollable loads using optimal bidding strategies.

References

[1] J. Yan, L. Lu, T. Ma, Y. Zhou, C. Zhao, Thermal management of the waste energy of a stand-alone hybrid pv-wind-battery power system in hong kong, Energy Conversion and Management 203 (2020) 112261.

[2] A. Coelho, N. Neyestani, F. Soares, J. P. Lopes, Wind variability mitigation using multi-energy systems, International Journal of Electrical Power & Energy Systems 118 (2020) 105755.

[3] L. Kumar, M. Hasanuzzaman, N. Rahim, Global advancement of solar thermal energy technologies for industrial process heat and its future prospects: A review, Energy Conversion and Management 195 (2019) 885–908.

[4] EU, Directive 2009/28/EC of the European Parliament and of the Council of 23 April 2009 on the promotion of the use of energy from renewable sources and amending and subsequently repealing Directives 2001/77/EC and 2003/30/EC, Official Journal of the European Union (2009).

[5] A. R. Starke, J. M. Cardemil, R. Escobar, S. Colle, Multi-objective optimization of hybrid csp+ pv system using genetic algorithm, Energy 147 (2018) 490–503.

[6] R. Secretariat, Renewables 2020 global status report, Renewables Global Status Report (GSR) (2020).

[7] P. Jiang, J. Dong, H. Huang, Optimal integrated demand response scheduling in regional integrated energy system with concentrating solar power, Applied Thermal Engineering 166 (2020) 114754.

[8] K. Lovegrove, W. Stein, Concentrating solar power technology: principles, developments and applications, Elsevier, 2012.

[9] Z. Wang, X. Lin, N. Tong, Z. Li, S. Sun, C. Liu, Optimal planning of a 100% renewable energy island supply system based on the integration of a concentrating solar power plant and desalination units, International Journal of Electrical Power & Energy Systems 117 (2020) 105707.

[10] M. K. Koukou, M. G. Vrachopoulos, N. S. Tachos, G. Dogkas, K. Lymperis, V. Stathopoulos, Experimental and computational investigation of a latent heat energy storage system with a staggered heat exchanger for various phase change materials, Thermal Science and Engineering Progress 7 (2018) 87–98.

[11] H. Liu, B. Li, L. Zhang, X. Li, Optimizing heat-absorption efficiency of phase change materials by mimicking leaf vein morphology, Applied Energy 269 (2020) 114982.

[12] Q. Yu, X. Li, Z. Wang, Q. Zhang, Modeling and dynamic simulation of thermal energy storage system for concentrating solar power plant, Energy 198 (2020) 117183.

[13] M. T. Plytaria, C. Tzivanidis, E. Bellos, K. A. Antonopoulos, Parametric analysis and optimization of an underfloor solar assisted heating system with phase change materials, Thermal Science and Engineering Progress 10 (2019) 59–72.

[14] Z. Wang, S. Sun, X. Lin, C. Liu, N. Tong, Q. Sui, Z. Li, A remote integrated energy system based on cogeneration of a concentrating solar power plant and buildings with phase change materials, Energy Conversion and Management 187 (2019) 472–485.

[15] Y. Fang, S. Zhao, Risk-constrained optimal scheduling with combining heat and power for concentrating solar power plants, Solar Energy 208 (2020) 937–948.

[16] L. Tang, Y. Zhou, S. Zheng, G. Zhang, Exergy-based optimisation of a phase change materials integrated hybrid renewable system for active cooling applications using supervised machine learning method, Solar Energy 195 (2020) 514–526.

[17] EC, Directive 2004/8/EC of the European Parliament and of the Council of 11 February 2004 on the promotion of cogeneration based on a useful heat demand in the internal energy market and amending Directive 92/42/EEC, Official Journal of the European Union (2004).

[18] Y. Li, C. Wang, G. Li, J. Wang, D. Zhao, C. Chen, Improving operational flexibility of integrated energy system with uncertain renewable generations considering thermal inertia of buildings, Energy Conversion and Management 207 (2020) 112526.

[19] D. Pudjianto, C. Ramsay, G. Strbac, Virtual power plant and system integration of distributed energy resources, IET Renewable power generation 1 (1) (2007) 10–16.

[20] M. Fan, V. Vittal, G. T. Heydt, R. Ayyanar, Probabilistic power flow studies for transmission systems with photovoltaic generation using cumulants, IEEE Transactions on Power Systems 27 (4) (2012) 2251–2261.

[21] D. Yu, A. G. Ebadi, K. Jermsittiparsert, N. H. Jabarullah, M. V. Vasiljeva, S. Nojavan, Risk-constrained stochastic optimization of a concentrating solar power plant, IEEE Transactions on Sustainable Energy 11 (3) (2019) 1464–1472.

[22] K. Hu, L. Chen, Q. Chen, X. H. Wang, J. Qi, F. Xu, Y. Min, Phase-change heat storage installation in combined heat and power plants for integration of renewable energy sources into power system, Energy 124 (2017) 640–651.

[23] A. Chmielewski, J. Kupecki, Ł. Szabłowski, K. J. Fijałkowski, J. Zawieska, K. Bogdziński, O. Kulik, T. Adamczewski, Currently available and future methods of energy storage, WWF Poland (2020).

[24] Polityka Energetyczna Polski do 2040 roku - projekt. (Energy Policy of Poland until 2040 (EPP2040) - draft), Warsaw: Ministry of Energy (2019).

[25] C. Wan, J. Zhao, Y. Song, Z. Xu, J. Lin, Z. Hu, Photovoltaic and solar power forecasting for smart grid energy management, CSEE Journal of Power and Energy Systems 1 (4) (2015) 38–46.

[26] W. Yao, C. Xu, J. Zhao, X. Wang, Y. Wang, X. Li, J. Cao, The modified ashrae model based on the mechanism of multi-parameter coupling, Energy Conversion and Management 209 (2020) 112642.

[27] C. Yue, C. Chen, Y. Lee, Integration of optimal combinations of renewable energy sources into the energy supply of Wang-An Island, Renewable Energy 86 (2016) 930–942.

[28] F. Petrakopoulou, A. Robinson, M. Loizidou, Simulation and analysis of a stand-alone solar-wind and pumped-storage hydropower plant, Energy 96 (2016) 676–683.

[29] G. Notton, M. Nivet, C. Voyant, C. Paoli, C. Darras, F. Motte, A. Fouilloy, Intermittent and stochastic character of renewable energy sources: Consequences, cost of intermittence and benefit of forecasting, Renewable and sustainable energy reviews 87 (2018) 96–105.

[30] S. R. Salkuti, Multi-objective based economic environmental dispatch with stochastic solar-wind-thermal power system, International Journal of Electrical & Computer Engineering (2088-8708) 10 (5) (2020).

[31] K. Huang, P. Liu, B. Ming, J. Kim, Y. Gong, Economic operation of a wind-solar-hydro complementary system considering risks of output shortage, power curtailment and spilled water, Applied Energy 290 (2021) 116805.

[32] J. Jurasz, A. Kies, P. Zajac, Synergetic operation of photovoltaic and hydro power stations on a day-ahead energy market, Energy 212 (2020) 118686.

[33] Q. Yan, B. Zhang, M. Kezunovic, Optimized operational cost reduction for an ev charging station integrated with battery energy storage and pv generation, IEEE Transactions on Smart Grid 10 (2) (2018) 2096–2106.

[34] D. Cocco, L. Migliari, M. Petrollese, A hybrid csp–cpv system for improving the dispatchability of solar power plants, Energy Conversion and Management 114 (2016) 312–323.

[35] K. Rashid, K. Mohammadi, K. Powell, Dynamic simulation and techno-economic analysis of a concentrated solar power (csp) plant hybridized with both thermal energy storage and natural gas, Journal of Cleaner Production 248 (2020) 119193.

[36] Y. Yang, S. Guo, D. Liu, R. Li, Y. Chu, Operation optimization strategy for wind-concentrated solar power hybrid power generation system, Energy Conversion and Management 160 (2018) 243–250.

[37] Y. Fang, S. Zhao, Look-ahead bidding strategy for concentrating solar power plants with wind farms, Energy (2020) 117895.

[38] R. Dominguez, L. Baringo, A. Conejo, Optimal offering strategy for a concentrating solar power plant, Applied Energy 98 (2012) 316–325.

[39] G. He, Q. Chen, C. Kang, Q. Xia, Optimal offering strategy for concentrating solar power plants in joint energy, reserve and regulation markets, IEEE Transactions on sustainable Energy 7 (3) (2016) 1245–1254.

[40] M. Yazdani-Damavandi, N. Neyestani, G. Chicco, M. Shafie-Khah, J. P. Catalao, Aggregation of distributed energy resources under the concept of multienergy players in local energy systems, IEEE Trans. Sustainable Energy 8 (4) (2017) 1679–1693.

[41] H. Pandžić, J. M. Morales, A. J. Conejo, I. Kuzle, Offering model for a virtual power plant based on stochastic programming, Applied Energy 105 (2013) 282–292.

[42] R. Shan, A. Abdulla, M. Li, Deleterious effects of strategic, profit-seeking energy storage operation on electric power system costs, Applied Energy 292 (2021) 116833.

[43] S. Wu, C. Zhou, E. Doroodchi, B. Moghtaderi, Thermodynamic analysis of a novel hybrid thermochemical-compressed air energy storage system powered by wind, solar and/or off-peak electricity, Energy Conversion and Management 180 (2019) 1268–1280.

[44] D. Pudjianto, C. Ramsay, G. Strbac, M. Durstewitz, The virtual power plant: Enabling integration of distributed generation and demand, FENIX Bulletin 2 (2008) 10–16.

[45] E. Akbari, R. Hooshmand, M. Gholipour, M. Parastegari, Stochastic programming-based optimal bidding of compressed air energy storage with wind and thermal generation units in energy and reserve markets, Energy 171 (2019) 535–546.

[46] M. Abbaspour, M. Satkin, B. Mohammadi-Ivatloo, F. H. Lotfi, Y. Noorollahi, Optimal operation scheduling of wind power integrated with compressed air energy storage (caes), Renewable Energy 51 (2013) 53–59.

[47] E. G. Kardakos, C. K. Simoglou, A. G. Bakirtzis, Optimal bidding strategy in transmission-constrained electricity markets, Electric Power Systems Research 109 (2014) 141–149.

[48] X. Zhang, R. Zeng, Q. Deng, X. Gu, H. Liu, Y. He, K. Mu, X. Liu, H. Tian, H. Li, Energy, exergy and economic analysis of biomass and geothermal energy based cchp system integrated with compressed air energy storage (caes), Energy Conversion and Management 199 (2019) 111953.

[49] Y. Li, S. Miao, B. Yin, J. Han, S. Zhang, J. Wang, X. Luo, Combined heat and power dispatch considering advanced adiabatic compressed air energy storage for wind power accommodation, Energy Conversion and Management 200 (2019) 112091.

[50] X. Wang, C. Yang, M. Huang, X. Ma, Multi-objective optimization of a gas turbine-based cchp combined with solar and compressed air energy storage system, Energy conversion and management 164 (2018) 93–101.

[51] S. Pfenninger, L. Staffell, renewables and weather parameters-Renewables.ninja.
URL \textcolor{black}{https://www.renewables.ninja/}

[52] H. Heitsch, W. Römisch, Scenario reduction algorithms in stochastic programming, Computational optimization and applications 24 (2) (2003) 187–206.